Carcinogenesis, 2017, Vol. 38, No. 11, 1136–1146

doi:10.1093/carcin/bgx082
Advance Access publication September 23, 2017
Original Article

ORIGINAL ARTICLE

Herbacetin suppresses cutaneous squamous cell carcinoma and melanoma cell growth by targeting AKT and ODC

Dong Joon Kim[1,2,*], Mee-Hyun Lee[1], KangDong Liu[1,3,4,5], Do Young Lim[2], Eunmiri Roh[2], Hanyong Chen[2], Sung-Hyun Kim[1], Jung-Hyun Shim[6], Myoung Ok Kim[7], Wenwen Li[1], Fayang Ma[1], Mangaladoss Fredimoses[1], Ann M. Bode[2] and Zigang Dong[1,2]

[1]China-US (Henan) Hormel Cancer Institute, Zhengzhou, Henan 450008, China, [2]The Hormel Institute, University of Minnesota, Austin, MN 55912, USA, [3]The Pathophysiology Department, The School of Basic Medical Sciences, Zhengzhou University, Zhengzhou, Henan 450008, China, [4]The Affiliated Cancer Hospital, Zhengzhou University, Zhengzhou, Henan, China, [5]The Collaborative Innovation Center of Henan Province for Cancer Chemoprevention, Zhengzhou, China, [6]College of Pharmacy, Mokpo National University, Muan-gun, Jeonnam 534-729, Republic of Korea and [7]Center for Laboratory Animal Resources, School of Animal Biotechnology, Kyungpook National University, Dae-gu 700-842, Republic of Korea

*To whom correspondence should be addressed. Tel: +1 371 6558 7909; Fax: +1 507 437 9606; Email: djkim@hci-cn.org
Correspondence may also be addressed to Zigang Dong. Tel: +1 507 437 9600; Fax: +1 507 437 9606; Email: zgdong@hi.umn.edu

Abstract

Herbacetin is a flavonol compound that is found in plants such as flaxseed and ramose scouring rush herb, it possesses a strong antioxidant capacity, and exerts anticancer effects on colon and breast cancer. However, the effect of herbacetin on skin cancer has not been investigated. Herein, we identified herbacetin as a dual V-akt murine thymoma viral oncogene homolog (AKT) and ornithine decarboxylase (ODC) inhibitor, and illustrated its anticancer effects *in vitro* and *in vivo* against cutaneous squamous cell carcinoma (SCC) and melanoma cell growth. To identify the direct target(s) of herbacetin, we screened several skin cancer-related protein kinases, and results indicated that herbacetin strongly suppresses both AKT and ODC activity. Results of cell-based assays showed that herbacetin binds to both AKT and ODC, inhibits TPA-induced neoplastic transformation of JB6 mouse epidermal cells, and suppresses anchorage-independent growth of cutaneous SCC and melanoma cells. The inhibitory activity of herbacetin was associated with markedly reduced NF-κB and *AP1* reporter activity. Interestingly, herbacetin effectively attenuated TPA-induced skin cancer development and also exhibited therapeutic effects against solar–UV-induced skin cancer and melanoma growth *in vivo*. Our findings indicate that herbacetin is a potent AKT and ODC inhibitor that should be useful for preventing skin cancers.

Introduction

Skin cancer is the most common type of cancer and the incidence continues to increase by 1.3 million new cases each year in the United States (1). The non-melanoma skin cancers, including basal cell carcinomas (BCCs) and squamous cell carcinomas (SCCs), account for 80 and 16% of all skin cancers, respectively (2). The two-stage skin carcinogenesis mouse model initiated by chemical agents such as 7,12-dimethylbenzanthracene (DMBA) and promoted by 12-O-tetradecanoylphorbol 13-acetate (TPA) is used to study the initiation, promotion and progression of mouse skin tumors (3–5). Additionally, the solar ultraviolet (UV) irradiation-induced skin cancer mouse model is well-established. Although many environmental and genetic factors contribute to the development of skin cancer, the most important factor is chronic exposure of the skin to solar UV irradiation. TPA

Received: January 11, 2017; **Revised:** June 26, 2017; **Accepted:** August 3, 2017

Abbreviations

AKT	V-akt murine thymoma viral oncogene homolog
AP1	activator protein-1
DMBA	7,12-dimethylbenz[α]-anthracene
ERKs	extracellular signal-regulated kinases
NF-κB	nuclear factor-kappaB
RSK	ribosomal S6 kinase;
TPA	12-O-tetradecanoylphorbol-13-acetate

or solar UV induces high levels of polyamines, which correlate with skin cancer development (6). Increased polyamine levels are associated with increased cell growth, cell motility, metastasis and decreased apoptosis (6). Additionally, polyamines activate the phosphorylation of ERKs and induce the expression of oncogenes such as *myc*, *jun* and *fos* (7). Ornithine decarboxylase (ODC) is the first enzyme in the polyamine synthesis pathway, and elevated ODC activity has been observed in mouse skin papillomas, as compared to normal skin (8). Previous reports suggested highly correlative effects of ODC activities and polyamines in their ability to induce skin cancer caused by DMBA/TPA or solar UV irradiation (9,10). Additionally, fibroblast transformation induced by activated RAS induces ODC expression, and ODC promotes RAS-mediated skin carcinogenesis in mice (11,12). However, evidence has not been provided that implicates HRAS in the regulation of polyamine metabolic enzymes in epithelial cancers (12). DMBA treatment alone can induce skin tumor development in K6.ODC and K5.ODC mice (13). Furthermore, reduced ODC expression in heterozygous ODC-null mice strongly suppresses DMBA/TPA-induced skin tumorigenesis (14), indicating that overexpression of ODC is enough to cause tumorigenesis. Additionally, the V-akt murine thymoma viral oncogene homolog (AKT)-dependent signaling pathway is important in the early step of the two-stage skin carcinogenesis and MAPK signaling is most heavily involved in the later stages of malignant conversion (15). Therefore, these pathways represent key mechanisms in skin carcinogenesis. Furthermore, these pathways provide compensatory mechanisms because they cross-talk extensively to both positively and negatively regulate each other (16). Therefore, co-inhibition of both pathways has been successful in reducing tumor growth in *in vivo* models (17,18).

In melanoma, both the RAS/RAF/MEK/ERKs and PI3K/AKT signaling pathways are constitutively activated through multiple mechanisms (19). Over 50% of melanomas harbor activating mutations in the *BRAF* gene at V600E, which is known to play a key role in proliferation and survival of melanoma cells through the activation of the MAPK pathway (20,21). The PI3K/AKT (phosphatidylinositol 3-kinase/v-akt murine thymoma viral oncogene homologue) is one of the most frequently activated proliferation and survival pathways and is an important intracellular signaling pathway downstream of many growth factor receptors (22,23). The most frequent causes of changes in this pathway include mutation or increased gene copy numbers of *PIK3CA* or other PI3K isoforms, loss of expression of the pathway suppressors or hyperactivation of receptor tyrosine kinases through receptor overexpression or activating mutations (24–26). Although mutations in *AKT* genes are rarely found in skin cancers, aberrant AKT activation can occur through numerous mechanisms that affect elements upstream of AKT (27,28). Additionally, increased phosphorylation of AKT in melanoma is associated with tumor progression and shorter survival (29–31).

The transcription factor, nuclear factor-kappaB (NF-κB) is heavily involved in oncogenesis through its ability to control cell proliferation and survival in various cancers (32). This signaling cascade interacts with several parallel pathways, including the signaling cascades initiated by the PI3K/AKT signaling pathway (33). Previous findings suggested that the AKT-dependent interaction between IKK and mTOR positively regulates NF-κB activity (34,35). The NF-κB family of proteins is overexpressed in the nuclei of dysplastic nevi and melanoma cells compared to normal nevi and healthy melanocytes (36). Therefore, targeting AKT and ODC are a potential strategy for cancer chemoprevention and chemotherapy against skin cancer.

Herbacetin is a flavonol compound that is found in plants such as flaxseed and ramose scouring rush herb (37) and it possesses a strong antioxidant capacity and exerts anticancer effects against breast cancer and colon cancer (38,39). Previous findings indicated that herbacetin increased cellular apoptosis by inducing reactive oxygen species (ROS) and reducing PI3K/AKT signaling in hepatocellular carcinoma hepG2 cells (40). It also suppressed hepatocyte growth factor-induced cell motility by inhibiting c-Met and AKT signaling in breast cancer cells (38). Recently, herbacetin was identified as an allosteric ornithine decarboxylase (ODC) inhibitor that effectively suppressed colon tumor growth (39). However, its biological functions and activities are still not completely elucidated in other cancers. In the present study, we investigated the anticancer effects of herbacetin against DMBA/TPA-solar UV-induced skin carcinogenesis and melanoma xenograft growth *in vivo* and found that herbacetin is a novel AKT and ODC inhibitor that can attenuate skin carcinogenesis.

Materials and methods

Cell lines

Cell lines were purchased from American Type Culture Collection (ATCC) and were cytogenetically tested and authenticated before being frozen. Each vial of frozen cells was thawed and maintained in culture for a maximum of 8 weeks. Enough frozen vials were available for each cell line to ensure that all cell-based experiments were conducted on cells that had been tested and in culture for 8 weeks or less. JB6 mouse epidermal cells were cultured in minimal Eagle's medium (MEM) supplemented with 5% fetal bovine serum (FBS; Atlanta Biologicals, Lawrenceville, GA) and 1% antibiotic-antimycotic. N/TERT-1 human skin cells were purchased from the Harvard Skin Disease Research Center and cultured in bronchial epithelial cell basal medium (BEBM; Lonza, Portsmouth, NH) supplemented with gentamicin, bovine pituitary extract (BPE), transferrin, insulin, human recombinant epidermal growth factor (hrEGF), hydrocortisone and epinephrine. A431 human cutaneous SCC cells were cultured in Dulbecco's Modified Eagle's Medium (DMEM) supplemented with 10% FBS (Biological Industries, Cromwell, CT) and 1% antibiotic-antimycotic. SK-MEL-5 or -28 human melanoma cells were cultured in Minimal Essential Medium with Earle's Balanced Salts (MEM/EBSS) supplemented with 10% FBS (Biological Industries) and 1% antibiotic-antimycotic.

Reagents and antibodies

Herbacetin (purity: > 90% by HPLC) was purchased from Indofine Chemical Company (Hillsborough, NJ). CNBr-Sepharose 4B beads were from GE Healthcare (Piscataway, NJ). Antibodies to detect total ERKs, phosphorylated ERKs (T202/Y204), total RSK, phosphorylated RSK (S380), total AKT, phosphorylated AKT (S473), total p65 and phosphorylated p65 (S536) were purchased from Cell Signaling Technology (Beverly, MA). The antibody to detect β-actin was from Santa Cruz Biotechnology (Santa Cruz, CA).

Anchorage-independent cell growth

Cells (8×10^3 per well) suspended in complete growth medium (Basal Medium Eagle; BME) supplemented with FBS (5% FBS for JB6 cells, 10% FBS for cutaneous SCC and melanoma cells) were added to 0.3% agar with or without TPA, and different concentrations of herbacetin in a top layer over a base layer of 0.6% agar with or without TPA and different concentrations

of herbacetin. The cultures were maintained at 37°C in a 5% CO_2 incubator for 2 weeks and then colonies were counted under a microscope using the Image-Pro Plus software (v.6) program (Media Cybernetics).

Luciferase assay for reporter activity

The reporter activity assay was conducted according to the manufacturer's manual (Promega, Madison, WI). *AP1*- or *NF*-κB-stably transfected JB6 cells (1×10^4 per well) were seeded on 12-well culture plates and incubated for 24 h. Cells were cultured in 0.1% FBS/MEM for 24 h and then treated with herbacetin for 2 h before treatment with TPA for 48 h. Cutaneous SCC or melanoma cells were seeded on 12-well culture plates and incubated for 24 h. Cells were transfected with the *AP1* or *NF*-κB reporter plasmid for 24 h and treated with herbacetin for 48 h. Cells were harvested in Promega Lysis Buffer. The luciferase and *Renilla* activities were measured using substrates in the reporter assay system (Promega). The luciferase activity was normalized to *Renilla* activity.

ODC enzyme assay

ODC activity was measured as the release of CO_2 from L-[1-^{14}C] ornithine as previously described (39).

Cell viability assay

To estimate viability, cells were seeded (6×10^3 cells/well) in 96-well plates with BEBM at 37°C in a 5% CO_2 incubator. The cells were treated with herbacetin at various concentrations for 24 or 48 h. After incubation, 20 μl of MTT solution (Solarbio, Beijing, China) were added to each well, and the cells were then incubated for 1 h at 37°C in a 5% CO_2 incubator. Absorbance was measured at 570 nm.

Cell proliferation assay

Cells were seeded (1×10^3 cells per well) in 96-well plates and incubated for 24 h. JB6 cells were cultured in 0.1% FBS/MEM for 24 h and then treated with TPA and different concentrations of herbacetin. N/TERT-1, A431, SK-MEL-5 or -28 cells were seeded (2×10^3 cells per well) in 96-well plates and incubated for 24 h. Cells were treated with different concentrations of herbacetin. After incubation for 48 h, 20 μl of CellTiter96 Aqueous One Solution (Promega) were added and then cells were incubated for 1 h at 37°C in a 5% CO_2 incubator. Absorbance was measured at 492 nm.

Pull-down assay using CNBr-herbacetin-conjugated beads

Total cell lysates (500 μg) were incubated with herbacetin-Sepharose 4B (or Sepharose 4B only as a control) beads (50 μl, 50% slurry). The pull-down assay was described previously (39).

Computational modeling of AKT1, AKT2 and ODC with herbacetin

For *in silico* docking with herbacetin and AKTs, we used the Schrödinger Suite 2015 software programs. AKT1 and AKT2 crystal structures were first derived from the PDB Bank (41) and then they were prepared under the standard procedures of the Protein Preparation Wizard (Schrödinger Suite 2015). Hydrogen atoms were added consistent with a pH of 7 and all water molecules removed. The AKT1 and AKT2 ATP-binding site-based receptor grid was generated for docking, and also ODC-allosteric binding site was generated as previously described (39). Herbacetin was prepared for docking by default parameters using the LigPrep program. Then, the docking of herbacetin with ODC, AKT1 and AKT2 was accomplished with default parameters under the extra precision (XP) mode using the program Glide, respectively. Herein, we could get the best-docked representative structures.

In vivo studies using the DMBA/TPA two-stage skin carcinogenesis mouse model

Hairless SKH:HR-1-hrBr (SKH-1) mice were obtained from Charles River and maintained following the guidelines established by the University of Minnesota Institutional Animal Care and Use Committee. Mice (8–9 weeks old) were divided into five groups: (1) DMBA + vehicle group (n = 20); (2) DMBA-initiated (200 nmol) and TPA-promoted group (17 nmol; n = 20); (3) DMBA/TPA + 100 nmol of herbacetin (n = 20) group; (4) DMBA/TPA + 500 nmol of herbacetin group (n = 20); (5) DMBA + 500 nmol of herbacetin group (n = 20). One week after initiation with DMBA, 17 nmol of TPA in acetone was topically applied twice weekly until the termination of the experiment at 20 weeks. When used, each dose of herbacetin was dissolved in 0.2 ml of 10% H_2O in acetone and then topically applied to dorsal mouse skin at 30 min before TPA treatment. The number and volume of tumors per mouse was recorded weekly. The results are expressed as the percent of mice with tumors (incidence), average tumor volume (size) and average number of tumors per mouse (multiplicity).

In vivo studies using the solar–UV induced-skin tumor mouse model

Mice were exposed to solar–UV (48 kJ/UVA/2.9 kJ/UVB) three times weekly for 12 weeks. The solar UV treatment was discontinued and 20 weeks later, mice were topically treated with 100 or 500 nmol of herbacetin (in acetone) for an additional 7 weeks. Mice were treated with herbacetin or vehicle, five times per week. Mice (8~9 weeks old) were divided into three groups: (1) solar UV + vehicle group (n = 4); (2) solar UV + 100 nmol of herbacetin (n = 4) group; (3) solar UV + 500 nmol of herbacetin (n = 4). The weight and tumor volume per mouse were recorded weekly.

Xenograft mouse model

Athymic mice [Cr:NIH(S), NIH Swiss nude, 6–9-wk-old] were obtained from Charles River and maintained under 'specific pathogen-free' conditions based on the guidelines established by Zhengzhou University Institutional Animal Care and Use Committee. Mice were divided into three groups of eight animals each as follows: (1) untreated vehicle group; (2) 0.2 mg herbacetin/kg of body weight and (3) 1 mg herbacetin/kg body weight. SK-MEL-5 cells (3×10^6 cells/100 μl) were suspended in serum free MEM/EBSS medium including 50% Matrigel, and inoculated subcutaneously into the right flank of each mouse. Herbacetin or vehicle (5% DMSO in 10% tween 80) was injected three times per week for 15 days. Tumor volume was calculated from measurements of 2 diameters of the individual tumor base using the following formula: tumor volume (mm^3) = (length × width × height × 0.52). Mice were monitored until tumors reached 1 cm^3 total volume, at which time mice were euthanized and tumors extracted.

Hematoxylin–eosin staining and immunohistochemistry

Tumor tissues from mice were embedded in paraffin blocks and subjected to hematoxylin and eosin (H&E) staining and immunohistochemistry (IHC). Tissue sections were deparaffinized and hydrated, and then permeabilized with 0.5% Triton X-100/1 wiPBS for 10 min. After developing with 3, 3′-diaminobenzidine, the sections were counterstained with H&E. For IHC, sections were hybridized with the primary antibody (1:500) and a horse-radish peroxidase (HRP)-conjugated goat anti-rabbit or mouse IgG antibody was used as the secondary antibody. All sections were observed by microscope and the Image-Pro Plus software (v. 6) program (Media Cybernetics).

Statistical analysis

All quantitative results are expressed as mean values ± SD or ± SE. Significant differences were compared using the Student's t test or one-way analysis of variance (ANOVA). A P value of < 0.05 was considered to be statistically significant. The statistical software package used was the 'Statistical Package for the Social Sciences (SPSS Inc.)'.

Results

Herbacetin is a potent dual inhibitor of *AKT1/2 and ODC*

To identify potential molecular targets of herbacetin, we screened the effect of herbacetin against several PI3K-AKT signaling kinases using an *in vitro* kinase assay. The results indicated that AKT1 or AKT2 activity is inhibited by herbacetin (Figure 1A). Furthermore, quercetin and kaempferol have a similar structure

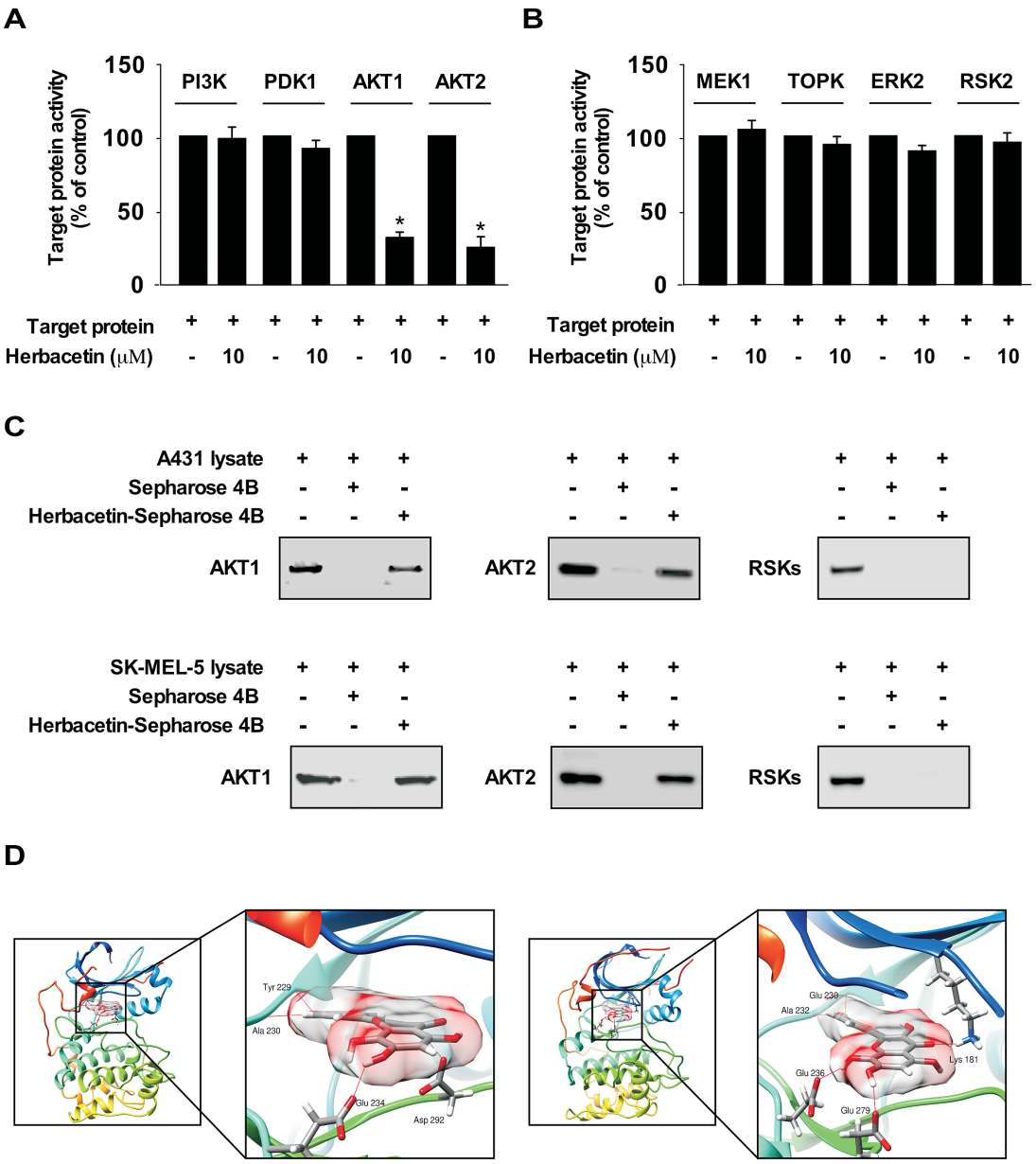

Figure 1. Herbacetin binds to AKT1/2 and suppresses each respective kinase activity. The effect of herbacetin on (**A**) PI3K/AKT and (**B**) MAPK signaling pathway proteins was determined by *in vitro* kinase assays using recombinant proteins. Data are shown as means ± S.D. of duplicate values from three independent experiments and the asterisk (*) indicates a significant ($P < 0.05$) effect of herbacetin compared to untreated controls. (**C**) Herbacetin binds to AKT1 or AKT2. A431 (cutaneous SCC) or SK-MEL-5 (melanoma) cell lysates were incubated with herbacetin-conjugated Sepharose 4B beads or Sepharose 4B beads alone. Proteins were pulled down and then analyzed by Western blotting using antibodies to detect AKT1, AKT2 or RSK. Similar results were observed from three independent experiments. (**D**) Modeling of herbacetin binding with AKT1 (left panel) or AKT2 (right panel). AKT1 and AKT2 structures are shown as ribbon representations. Herbacetin is shown as sticks with 60% surface transparency. Hydrogen bonds are shown as red lines.

to herbacetin, and have been reported to be a potent MEKs or RSK2 inhibitor, respectively. Therefore, to determine whether herbacetin has an effect on MAPK signaling, we performed an *in vitro* kinase assay using herbacetin. Results showed that herbacetin had little effect against these kinases (Figure 1B). Next, to examine the interaction between herbacetin and AKT1 or 2, we performed *in vitro* pull-down assays using herbacetin-conjugated Sepharose 4B beads (or Sepharose 4B as a negative control) and A431 (cutaneous SCC) and SK-MEL-5 (melanoma) cell lysates. Results showed that herbacetin directly binds to AKT1 or 2, but not RSKs in cells (Figure 1C). To better understand how herbacetin interacts with AKT1 or AKT2, we docked it into the ATP binding pocket of AKT1 or AKT2 using several protocols in the Schrödinger Suite 2015. From the docking model, we found that herbacetin formed hydrogen bonds with AKT1 or AKT2 (Figure 1D). These results indicated that herbacetin is a potential inhibitor of AKT1 or AKT2. Images were generated with the UCSF Chimera program (42). The inhibition of ODC activity, and its binding with herbacetin, and the computer modeling were described previously (39).

Anticancer activity of herbacetin

To evaluate the effect of herbacetin on cell viability, we treated N/TERT normal skin cells with herbacetin. Results showed that

herbacetin (50 μM concentration) had little effect on N/TERT cell viability (Figure 2A). To examine the effect of herbacetin on TPA-induced cell growth, JB6 cells were co-treated with herbacetin and TPA for 48 h. Results indicated that herbacetin significantly suppressed TPA-induced cell growth (Figure 2B) as well as cutaneous SCC and melanoma cell growth (Figure 2C). Additionally, to determine the effect of herbacetin on TPA-induced neoplastic cell transformation, cells were co-treated with TPA and herbacetin and results indicated that herbacetin markedly suppressed TPA-induced neoplastic transformation of JB6 epidermal cells (Figure 2D). Additionally, herbacetin strongly inhibited anchorage-independent cell growth in cutaneous SCC or melanoma cells (Figure 2E).

Herbacetin inhibits TPA-induced AP1 and NF-κB activity by suppressing AKT and ODC signaling in JB6 cells

We investigated whether herbacetin could directly affect the phosphorylation of GSK3β, which is a downstream signal for the AKT proteins. JB6 cells were treated with TPA for 15 min after pre-treatment with herbacetin for 2 h, and protein expression was analyzed by Western blotting. Results indicated that herbacetin strongly inhibits TPA-induced phosphorylation of GSK3β, but had no effect on ERKs, RSK or ODC (Figure 3A). Next, we determined whether TPA-induced ODC activity is regulated by herbacetin in JB6 mouse epidermal cells. Cells were treated with TPA for 24 h after pre-treatment with herbacetin for 2 h and ODC

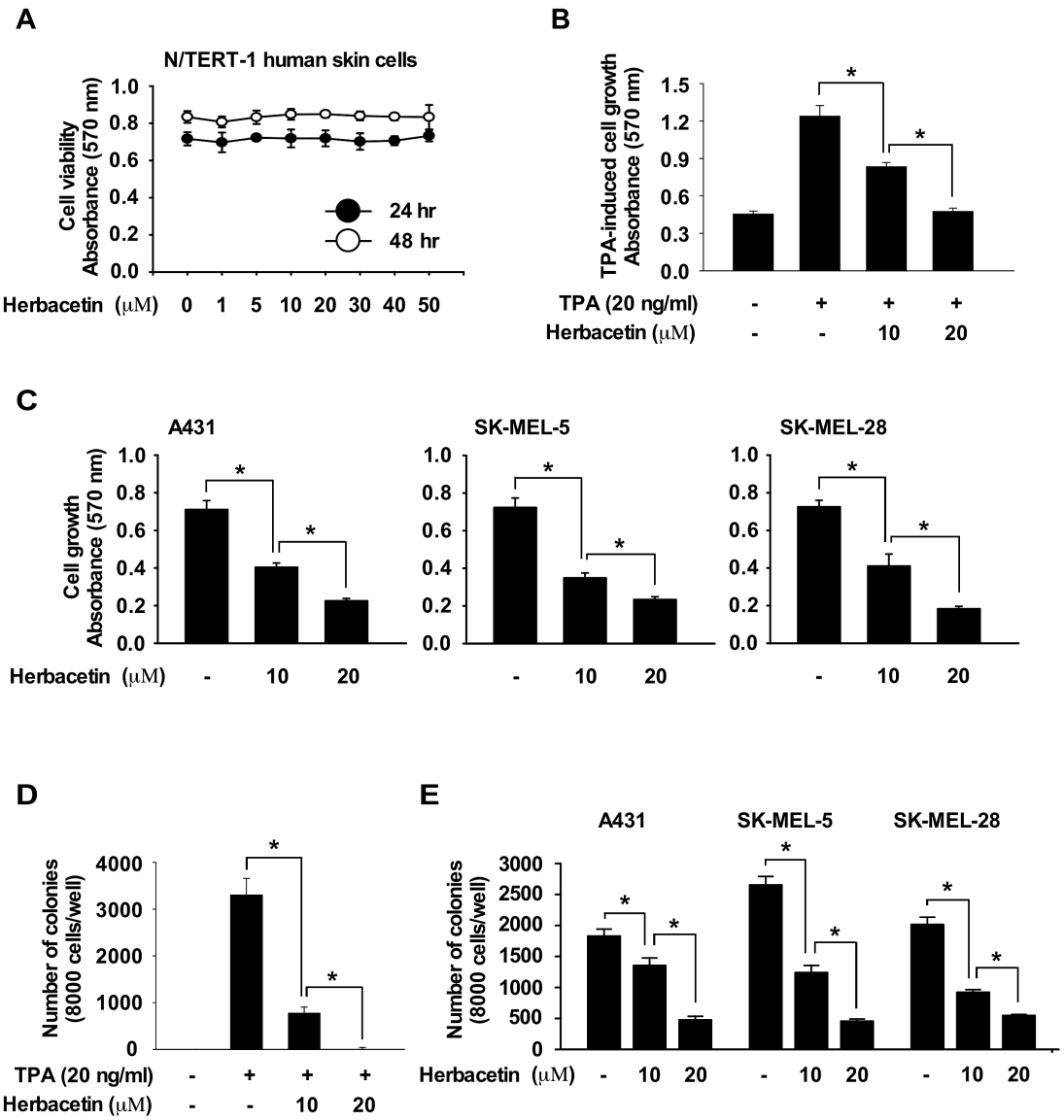

Figure 2. Anti-cancer effects are exerted by herbacetin. (**A**) Effect of herbacetin on viability of normal skin cells. Cells were treated with herbacetin for 24 or 48 h. Cell viability was measured at an absorbance of 570 nm. (**B**) Effect of herbacetin on TPA-induced growth of JB6 cells. TPA-induced cells were treated with herbacetin at various doses and then incubated for 48 h. (**C**) Effect of herbacetin on cutaneous SCC cell or melanoma cell growth. Cells were treated with herbacetin at various concentrations and then incubated for 48 h. For B and C, cell growth was estimated at 570 nm. (**D**) Effect of herbacetin on TPA-induced JB6 cell transformation. Cells treated with TPA and herbacetin were incubated for 2 weeks. (**E**) Effect of herbacetin on anchorage-independent growth of cutaneous SCC cells or melanoma cells. Cells were treated with herbacetin and incubated for 2 weeks. For D and E, colonies were counted using a microscope and the Image-Pro PLUS (v.6) computer software program. All data are shown as means ± SD. of triplicate values from three independent experiments and the asterisk (*) indicates a significant ($P < 0.05$) inhibitory effect of herbacetin on TPA-treated or untreated control cells compared to herbacetin-treated samples.

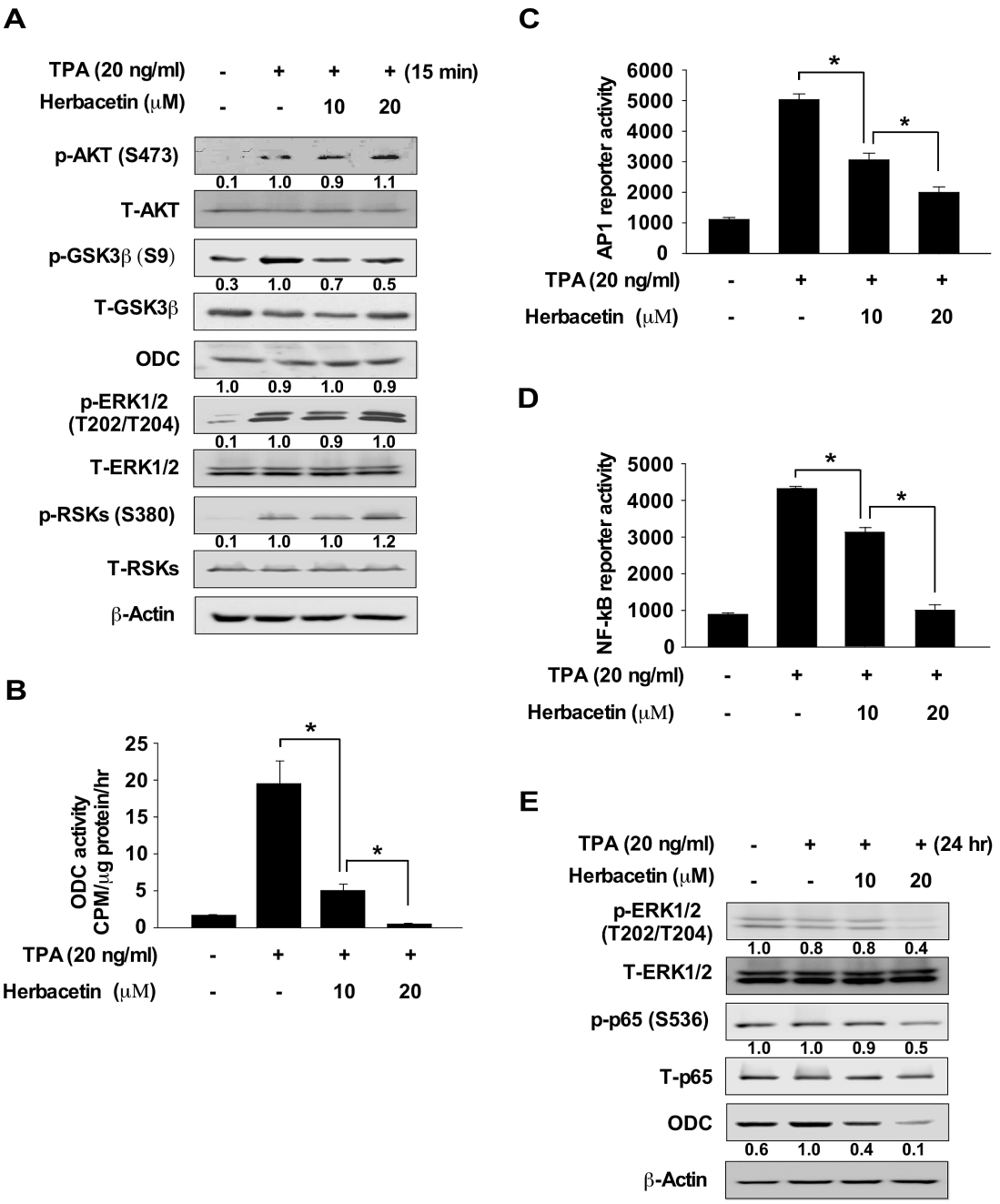

Figure 3. Herbacetin inhibits TPA-induced *AP1* or *NF-κB* promoter activity. (**A**) The effect of herbacetin on TPA-induced AKT and ERKs signaling. Serum-starved (0.1% FBS; 24 h) JB6 cells were treated with various doses of herbacetin for 1 h followed by treatment with TPA for 15 min. (**B**) Effect of herbacetin on TPA-induced ODC activity in JB6 cells. Serum-starved (0.1% FBS; 24 h) JB6 cells were treated with various doses of herbacetin for 1 h followed by treatment with TPA for 6 h. ODC activity was measured as the release of CO_2 from L-[1-^{14}C] ornithine. The effect of herbacetin on TPA-induced (**C**) *AP1* or (**D**) NF-κB reporter activity. Cells were treated with herbacetin and then incubated for 48 h. Reporter activity was measured using substrates included in the reporter assay system. Data are shown as means ± SD of triplicate values from three independent experiments and the asterisk (*) indicates a significant ($P < 0.05$) inhibitory effect of herbacetin on TPA-induced AP1 or NF-κB reporter activity. (**E**) The effect of herbacetin on TPA-induced phosphorylation of ERKs, p65 and ODC expression. JB6 cells were treated with various concentrations of herbacetin for 1 h followed by treatment with TPA for 24 h. For, A and E, cell lysates were analyzed by Western blotting. Similar results were obtained from three independent experiments.

activity was analyzed. Results showed that TPA-induced ODC activity was significantly suppressed by herbacetin (Figure 3B). Next, we determined whether herbacetin had an effect on activator protein-1 (*AP1*) and nuclear factor kappa B (*NF-κB*) reporter activity in JB6 cells stimulated with TPA. Cells were pre-treated with herbacetin for 2 h before stimulation with TPA for 48 h. *AP1* or *NF-κB* reporter activity was strongly suppressed by herbacetin through its inhibition of the phosphorylation of ERK1/2, p65 or ODC protein expression in TPA-treated JB6 cells (Figure 3C–E). These data suggested that herbacetin directly inhibited AKT and ODC activity resulting in attenuated *AP1* and *NF-κB* activation.

Herbacetin inhibits AP1 or NF-κB activity by suppressing AKT and ODC signaling in cutaneous SCC and melanoma cells

We also determined whether herbacetin affects phosphorylation of GSK3β in cutaneous SCC and melanoma cells. Cells were treated with herbacetin for 3 h and protein expression was

analyzed by Western blotting. Results showed that herbacetin suppresses phosphorylation of GSK3β, but does not affect ERKs phosphorylation and ODC protein expression (Figure 4A). Additionally, we determined whether ODC activity is regulated by herbacetin in cutaneous SCC or melanoma cells. Results indicated that herbacetin significantly inhibited ODC activity (Figure 4B). Furthermore, the cells were treated with herbacetin for 48 h to determine its effect on *AP1* or *NF-κB* reporter activity. Both reporter activities were significantly inhibited by herbacetin treatment in cutaneous SCC and melanoma cells. (Figure 4C and D).

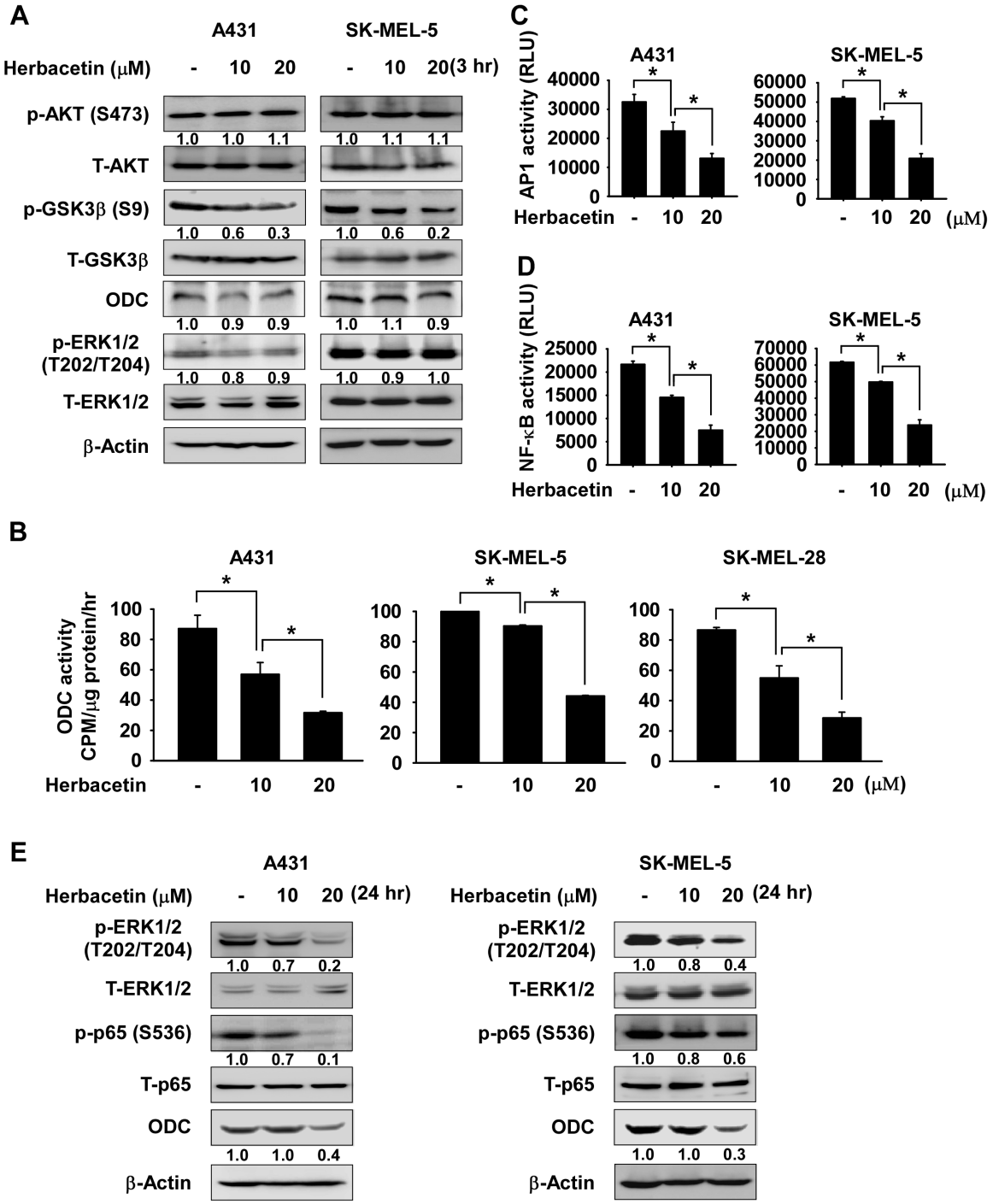

Figure 4. Herbacetin inhibits *AP1* or *NF-κB* activity in cutaneous SCC or melanoma cells. (**A**) The effect of herbacetin on AKT and ERKs signaling. Cells were treated with various concentrations of herbacetin for 3 h. (**B**) Effect of herbacetin on ODC activity in cutaneous SCC or melanoma cells. Cells were treated with various doses of herbacetin for 24 h and ODC activity was measured as the release of CO_2 from L-[1-^{14}C] ornithine. The effect of herbacetin on (**C**) *AP1* and (**D**) *NF-κB* reporter activity. Cells were treated with herbacetin and then incubated for 48 h. Reporter activity was measured using substrates included in the reporter assay system. Data are shown as means ± SD of triplicate values from three independent experiments and the asterisk (*) indicates a significant ($P < 0.05$) inhibitory effect of herbacetin on *AP1* or *NF-κB* reporter activity. (**E**) The effect of herbacetin on phosphorylated ERKs, p65 and ODC expression. Cells were treated with various concentrations of herbacetin for 24 h. For A and D, cell lysates were analyzed by Western blotting and similar results were obtained from three independent experiments.

Furthermore, phosphorylation of ERK1/2, p65 and ODC expression were also decreased in a dose-dependent manner (Figure 4E).

Herbacetin attenuates TPA-induced skin carcinogenesis and solar–UV-induced skin cancer *in vivo*

We examined the antitumor activity of herbacetin against skin carcinogenesis and its effectiveness in treating skin cancer using *in vivo* mouse models. We examined the effect of herbacetin on skin carcinogenesis in the two-stage 7,12-dimethylbenz[α]-anthracene (DMBA)/12-*O*-tetradecanoylphorbol-13-acetate (TPA)-induced skin cancer mouse model. Treatment of mice with herbacetin decreased the number and volume of skin papillomas relative to the TPA-only-treated group (Supplemental Figure 1A, available at *Carcinogenesis* Online; Figure 5A and B; $P < 0.05$). The compound also inhibited the phosphorylation of AKT and GSK3β as well as the expression of ODC downstream proteins, including ERKs and RSK (Figure 5C) and significantly attenuated ODC

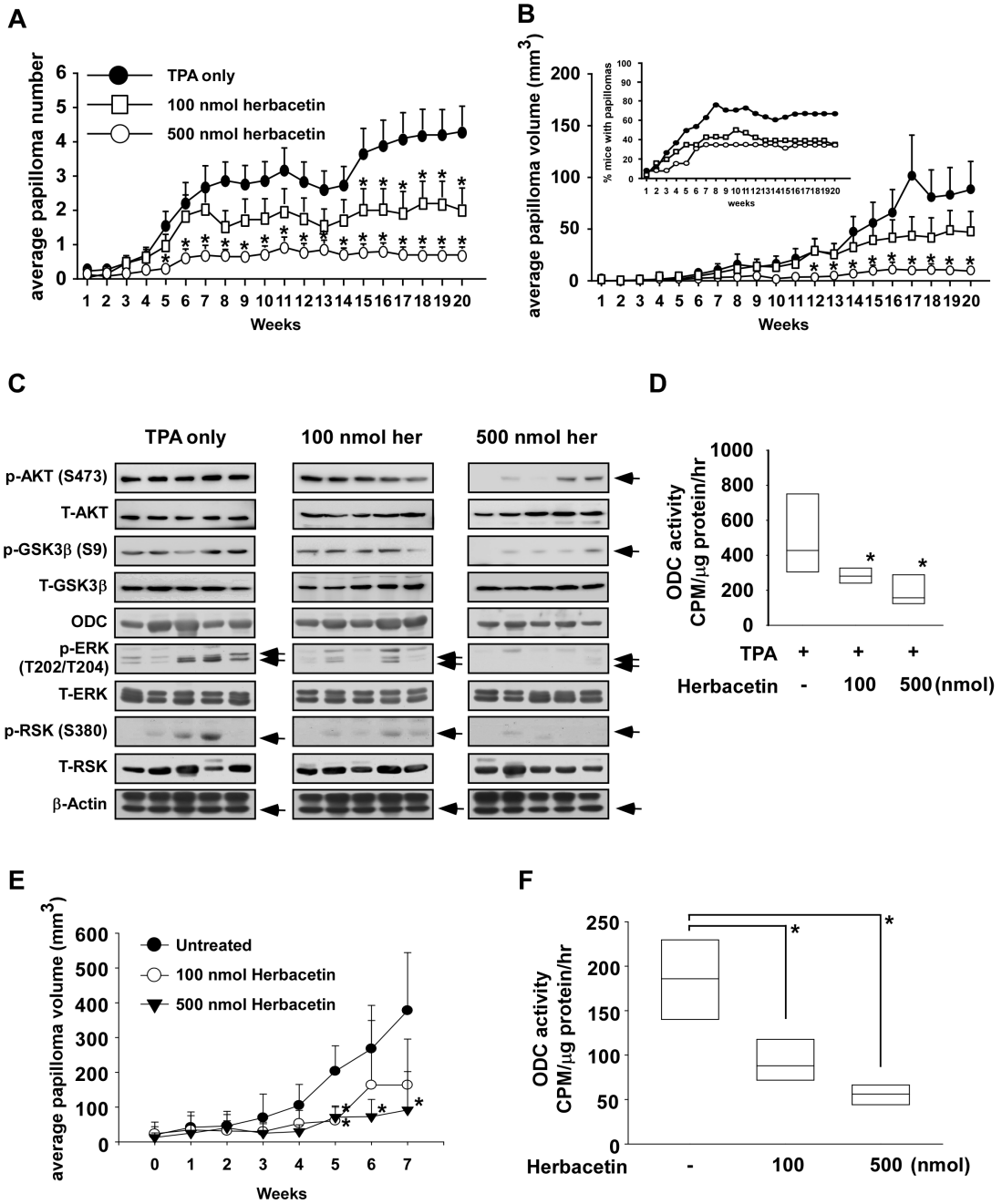

Figure 5. Herbacetin is a preventive and therapeutic agent against skin cancer *in vivo*. The effect of herbacetin on the (**A**) number and (**B**) volume of TPA-induced skin tumors was assessed weekly over 20 weeks. Data are shown as means ± SE of values ($n > 10$) and the asterisk (*) indicates a significant difference ($P < 0.05$) between herbacetin-treated groups compared to the TPA only-treated group. No tumors were observed in the vehicle-treated or the herbacetin only- (i.e. no TPA) treated groups. (**C**) Effect of herbacetin on AKT, ODC and ERKs signaling. (**D**) Measurement of ODC activity. Skin tissue tumors induced by TPA were isolated from vehicle- and herbacetin-treated groups of mice for immunoblot analysis of AKT and ERKs signaling. (**E**) The therapeutic effect of herbacetin (100 or 500 nmol) on solar UV-induced-mouse skin tumor volume was assessed weekly for 7 weeks (weeks 32–39). (**F**) Skin tissue tumors induced by solar–UV were isolated from vehicle- or herbacetin-treated groups of mice for measuring ODC activity. Data are shown as mean values ± SE and the asterisk (*) indicates a significant difference ($P < 0.05$) between herbacetin-treated groups compared to the vehicle-treated group.

activity (Figure 5D) *in vivo*. Furthermore, we examined the possible therapeutic effect of herbacetin on solar–UV-induced skin tumors in SKH-1 hairless mice. Tumors were induced by exposure of mice to solar UV for 12 weeks. Solar UV was discontinued to allow tumor development and 20 weeks later, tumors were treated with herbacetin (100 or 500 nmol) for an additional 7 weeks (Supplementary Figure 1B and C, available at *Carcinogenesis* Online). Results indicated that herbacetin significantly decreased the size (i.e., volume) of skin tumors relative to the vehicle group (Figure 5E; $P < 0.05$) as well as ODC activity (Figure 5F) *in vivo*.

Herbacetin suppresses melanoma tumor growth *in vivo*

Furthermore, we also examined the effects of herbacetin in a xenograft mouse model using SK-MEL-5 melanoma cells. These results indicated that herbacetin significantly decreased the volume of melanoma growth relative to the vehicle-treated group (Figure 6A; $P < 0.05$). Additionally, mice tolerated treatment with herbacetin without significant loss of body weight similar to the vehicle-treated group (Figure 6B). In addition, the effects of herbacetin on the Ki-67 tumor proliferation marker were evaluated

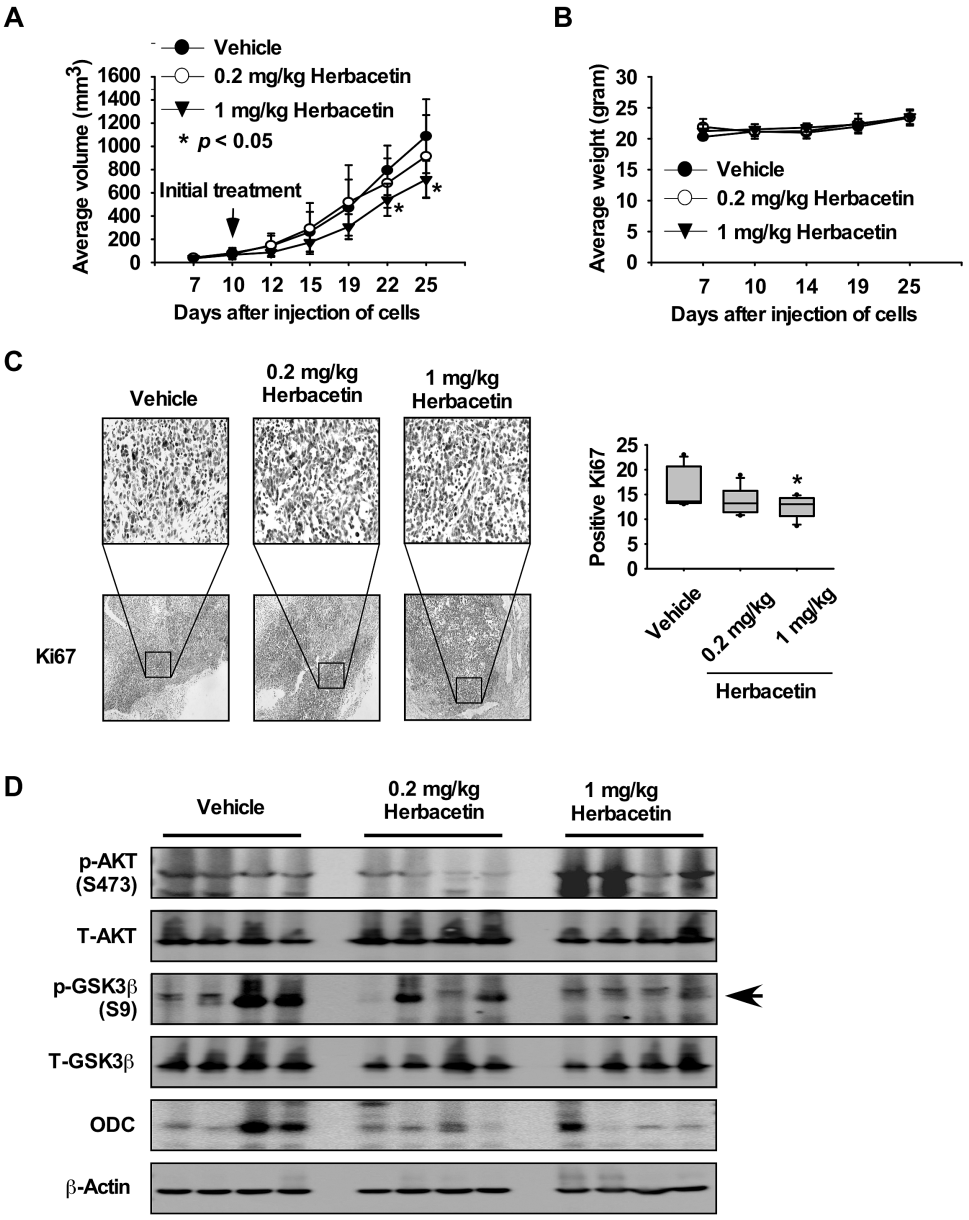

Figure 6. Herbacetin attenuates xenograft tumor growth. (**A**) Herbacetin suppresses melanoma tumor growth. SK-MEL-5 melanoma cells were injected subcutaneously into the dorsal right flank of mice. Mice were injected with herbacetin or vehicle three times a week for 15 days. Mice were monitored until tumors reached 1 cm^3 total volume at which time mice were euthanized and tumor tissues harvested. Tumor volume was calculated from measurements of 2 diameters of the individual tumor based on the following formula: tumor volume (mm^3) = (length × width × height × 0.52). Data are shown as means ± SE of values obtained from the experiments. The asterisk (*) indicates a significant difference between tumors from untreated or treated mice as determined by *t* test ($P < 0.05$). (**B**) Herbacetin has no effect on mouse body weight. Body weights from treated or untreated groups of mice were obtained once a week for 25 days. (**C**) Immunohistochemistry analysis of tumor tissues. Treated or untreated groups of mice were euthanized and tumor tissues harvested. Tumor tissue slides were prepared from paraffin sections after fixation with formalin and then stained with anti-Ki-67. Expression of Ki-67 was visualized by light microscope (×200). The number of Ki-67-stained cells (right panel) was counted from immunohistochemistry results ($N = 8$; *$P < 0.05$). (**D**) Herbacetin inhibits AKT and ODC signaling protein expression in melanoma tissues. Tumor tissues from groups treated with vehicle, 0.2 or 1 mg herbacetin per kg body weight were immunoblotted with antibodies to detect AKT, GSK3β, ERKs and β-actin.

in melanoma tissues by immunohistochemistry. The expression of Ki-67 was significantly decreased by treatment with herbacetin (Figure 6C). We then examined the effect of herbacetin on AKT1/2 phosphorylation, its downstream signaling and ODC protein expression in melanoma tissues. Results indicated that phosphorylation of GSK3β and ODC was suppressed by herbacetin treatment (Figure 6D). These findings indicated that melanoma growth was suppressed by herbacetin by targeting the AKT1/2 and ODC signaling pathway.

Discussion

Inhibitory effects of phytochemicals against carcinogenesis in animal models indicate that numerous cancers can be suppressed by the various functions, including antioxidant, anti-inflammatory and anti-carcinogenic properties, of these compounds (43). However, diet-based intervention and dietary prevention trials in humans have been disappointing (44–46). Although prevention of solar UV and carcinogen-induced skin carcinogenesis by various phytochemicals has been examined, their mechanism and direct targets have not been fully investigated.

In this study, we demonstrated in *in vitro* and cell-based assays that herbacetin is a potent AKT inhibitor. The AKT pathway is an important intracellular signaling pathway downstream of many growth factor receptors and its activation has been reported both in non-melanoma and in melanoma (47). In the DMBA/TPA two-stage skin carcinogenesis mouse model, AKT activity is increased during the promotion (20 weeks) and progression stages [30 weeks (15)]. Therefore, herbacetin seems to be working well during the promotion and progression stages of the DMBA/TPA mouse model (Figure 5A and C). Although many environmental and genetic factors contribute to the development of skin cancer, the most important etiologic factor is chronic exposure of the skin to solar UV irradiation. Therefore, we determined whether herbacetin could prevent solar UV-induced skin cancer. Our study showed that herbacetin strongly suppresses papilloma number and volume in solar UV-induced skin cancer mouse model and also attenuated SK-MEL-5 melanoma cell-induced tumor growth in a xenograft mouse model (Figures 5E and 6A). These findings suggested that herbacetin is a potent chemopreventive and chemotherapeutic compound.

Previous reports suggested that TPA or solar UV induces high level of polyamines, which correlate with skin cancer development (7,48,49). Increased polyamine levels are associated with increased cell growth, cell motility, metastasis and decreased apoptosis (7). ODC is the first enzyme in the polyamine synthesis pathway and elevated ODC activity has been observed in mouse skin papillomas compared to normal skin (8). Additionally, highly correlative effects of ODC activities and polyamines in their ability to induce skin cancer caused by DMBA/TPA or solar UV irradiation have been reported (9,10). Recently, our group showed that herbacetin was a novel allosteric inhibitor of ODC, and suppressed colon tumor growth (39). To determine the effects of herbacetin on ODC expression and activity, DMBA/TPA-induced skin tumor tissues were analyzed by Western blot and ODC activity was assessed. Results suggested that ODC protein expression and activity were strongly decreased by herbacetin treatment (Figure 5C and D). Furthermore, to identify more effective ODC inhibitor, we performed an *in vitro* ODC enzyme assay with herbacetin and 5 similar polyphenol compounds (quercetin, kaempferol, resveratrol, taxifolin and 7,3′,4′-trihydroxyisoflavone). Results showed that herbacetin and 7,3′,4′-trihydroxy-isoflavone most strongly inhibited ODC activity compared to other compounds (Supplementary Figures 2 and 3A, available at *Carcinogenesis* Online). Next, to confirm the effect of herbacetin or 7,3′,4′-trihydroxyisoflavone on ODC activity, we performed an *in vitro* ODC enzyme assay using these compounds in a dose-dependent manner. Results indicated that herbacetin was the most effective ODC inhibitory compound (Supplementary Figure 3B, available at *Carcinogenesis* Online).

The transcription factor, activator protein 1 (AP1), and the nuclear factor-kappaB (NF-κB) are heavily involved in oncogenesis through their ability to control cell proliferation and tumor progression in various cancers (32,50). Polyamines activate the phosphorylation of ERKs and induce the expression of AP1 components such as *jun,* and *fos* (7). Additionally, AKT could induce NF-κB activation through the phosphorylation of the RelA/p65 NF-κB subunit (34,51). Therefore, we investigated whether herbacetin suppresses AP1 and NF-κB activity. Our results suggested that herbacetin inhibited skin tumor growth by blocking the activation of AP1 and NF-κB through the suppression of ODC and AKT activity (Figures 3C and D; 4C and D).

Our findings support the idea that herbacetin is a potent AKT and ODC inhibitor that could be useful for preventing and treating skin cancers. Additional studies are planned to further characterize herbacetin, and perform pharmacokinetics and pharmacodynamics studies as well as elucidating toxicological responses.

Supplementary material

Supplementary material is available at *Carcinogenesis* online.

Funding

This work was supported by The Hormel Foundation and National Institutes of Health grants CA166011, CA187027, CA196639 and CA027502.

Acknowledgements

D.J.K. designed and performed the *in vitro* and *in vivo* experiments and prepared the manuscript; M-H.L., K.L., D.Y.L., F.M. and M.F. assisted with the experiments in the *in vivo* DMBA/TPA skin carcinogenesis and xenograft mouse model, H.C performed the computer modeling; E.R., S-H.K., J-H.S., M.O.K. and W.L assisted with the cell based assays; A.M.B. supervised the *in vivo* experimental design and manuscript editing; Z.D. provided the idea, supervised the overall experimental design and data analysis.
Conflict of Interest Statement: None declared.

References

1. Jemal, A. *et al.* (2005) Cancer statistics, 2005. CA. Cancer J. Clin., 55, 10–30.
2. Lomas, A. *et al.* (2012) A systematic review of worldwide incidence of nonmelanoma skin cancer. Br. J. Dermatol., 166, 1069–1080.
3. Fischer, S.M. *et al.* (1982) Inhibition of mouse skin tumor promotion by several inhibitors of arachidonic acid metabolism. Carcinogenesis, 3, 1243–1245.
4. Pashko, L.L. *et al.* (1984) Dehydroepiandrosterone (DHEA) and 3 beta-methylandrost-5-en-17-one: inhibitors of 7,12-dimethylbenz[a]anthracene (DMBA)-initiated and 12-O-tetradecanoylphorbol-13-acetate (TPA)-promoted skin papilloma formation in mice. Carcinogenesis, 5, 463–466.
5. Yuspa, S.H. (1998) The pathogenesis of squamous cell cancer: lessons learned from studies of skin carcinogenesis. J. Dermatol. Sci., 17, 1–7.
6. Gerner, E.W. *et al.* (2004) Polyamines and cancer: old molecules, new understanding. Nat. Rev. Cancer, 4, 781–792.

7. Bachrach, U. *et al.* (2001) Polyamines: new cues in cellular signal transduction. News Physiol. Sci., 16, 106–109.
8. O'Brien, T.G. (1976) The induction of ornithine decarboxylase as an early, possibly obligatory, event in mouse skin carcinogenesis. Cancer Res., 36(7 PT 2), 2644–2653.
9. Fischer, S.M. *et al.* (2001) Difluoromethylornithine is effective as both a preventive and therapeutic agent against the development of UV carcinogenesis in SKH hairless mice. Carcinogenesis, 22, 83–88.
10. Weeks, C.E. *et al.* (1982) alpha-Difluoromethylornithine, an irreversible inhibitor of ornithine decarboxylase, inhibits tumor promoter-induced polyamine accumulation and carcinogenesis in mouse skin. Proc. Natl. Acad. Sci. USA, 79, 6028–6032.
11. Shantz, L.M. *et al.* (1998) Ornithine decarboxylase induction in transformation by H-Ras and RhoA. Cancer Res., 58, 2748–2753.
12. Smith, M.K. *et al.* (1998) Co-operation between follicular ornithine decarboxylase and v-Ha-ras induces spontaneous papillomas and malignant conversion in transgenic skin. Carcinogenesis, 19, 1409–1415.
13. O'Brien, T.G. *et al.* (1997) Ornithine decarboxylase overexpression is a sufficient condition for tumor promotion in mouse skin. Cancer Res., 57, 2630–2637.
14. Guo, Y. *et al.* (2005) Haploinsufficiency for odc modifies mouse skin tumor susceptibility. Cancer Res., 65, 1146–1149.
15. Segrelles, C. *et al.* (2002) Functional roles of Akt signaling in mouse skin tumorigenesis. Oncogene, 21, 53–64.
16. Mendoza, M.C. *et al.* (2011) The Ras-ERK and PI3K-mTOR pathways: cross-talk and compensation. Trends Biochem. Sci., 36, 320–328.
17. Posch, C. *et al.* (2013) Combined targeting of MEK and PI3K/mTOR effector pathways is necessary to effectively inhibit NRAS mutant melanoma *in vitro* and *in vivo*. Proc. Natl. Acad. Sci. USA, 110, 4015–4020.
18. Ebi, H. *et al.* (2013) PI3K regulates MEK/ERK signaling in breast cancer via the Rac-GEF, P-Rex1. Proc. Natl. Acad. Sci. USA, 110, 21124–21129.
19. Strickland, L.R. *et al.* (2015) Targeting drivers of melanoma with synthetic small molecules and phytochemicals. Cancer Lett., 359, 20–35.
20. Garnett, M.J. *et al.* (2004) Guilty as charged: B-RAF is a human oncogene. Cancer Cell, 6, 313–319.
21. Davies, H. *et al.* (2002) Mutations of the BRAF gene in human cancer. Nature, 417, 949–954.
22. Manning, B.D. *et al.* (2007) AKT/PKB signaling: navigating downstream. Cell, 129, 1261–1274.
23. Altomare, D.A. *et al.* (2005) Perturbations of the AKT signaling pathway in human cancer. Oncogene, 24, 7455–7464.
24. Janku, F. *et al.* (2012) PIK3CA mutations in advanced cancers: characteristics and outcomes. Oncotarget, 3, 1566–1575.
25. Russo, A.E. *et al.* (2009) Melanoma: molecular pathogenesis and emerging target therapies (Review). Int. J. Oncol., 34, 1481–1489.
26. Zhao, J.J. *et al.* (2005) The oncogenic properties of mutant p110alpha and p110beta phosphatidylinositol 3-kinases in human mammary epithelial cells. Proc. Natl. Acad. Sci. USA, 102, 18443–18448.
27. Hafner, C. *et al.* (2010) Activation of the PI3K/AKT signalling pathway in non-melanoma skin cancer is not mediated by oncogenic PIK3CA and AKT1 hotspot mutations. Exp. Dermatol., 19, e222–e227.
28. Soung, Y.H. *et al.* (2006) Mutational analysis of AKT1, AKT2 and AKT3 genes in common human carcinomas. Oncology, 70, 285–289.
29. Niessner, H. *et al.* (2013) Targeting hyperactivation of the AKT survival pathway to overcome therapy resistance of melanoma brain metastases. Cancer Med., 2, 76–85.
30. Meier, F. *et al.* (2005) The RAS/RAF/MEK/ERK and PI3K/AKT signaling pathways present molecular targets for the effective treatment of advanced melanoma. Front. Biosci., 10, 2986–3001.
31. Dai, D.L. *et al.* (2005) Prognostic significance of activated Akt expression in melanoma: a clinicopathologic study of 292 cases. J. Clin. Oncol., 23, 1473–1482.
32. Hayden, M.S. *et al.* (2012) NF-κB, the first quarter-century: remarkable progress and outstanding questions. Genes Dev., 26, 203–234.
33. Romashkova, J.A. *et al.* (1999) NF-kappaB is a target of AKT in anti-apoptotic PDGF signalling. Nature, 401, 86–90.
34. Bai, D. *et al.* (2009) Akt-mediated regulation of NFkappaB and the essentialness of NFkappaB for the oncogenicity of PI3K and Akt. Int. J. Cancer, 125, 2863–2870.
35. Dan, H.C. *et al.* (2008) Akt-dependent regulation of NF-{kappa}B is controlled by mTOR and Raptor in association with IKK. Genes Dev., 22, 1490–1500.
36. McNulty, S.E. *et al.* (2004) Comparative expression of NFkappaB proteins in melanocytes of normal skin vs. benign intradermal naevus and human metastatic melanoma biopsies. Pigment Cell Res., 17, 173–180.
37. Struijs, K. *et al.* (2009) The chain length of lignan macromolecule from flaxseed hulls is determined by the incorporation of coumaric acid glucosides and ferulic acid glucosides. Phytochemistry, 70, 262–269.
38. Hyuga, S. *et al.* (2013) Herbacetin, a constituent of ephedrae herba, suppresses the HGF-induced motility of human breast cancer MDA-MB-231 cells by inhibiting c-Met and Akt phosphorylation. Planta Med., 79, 1525–1530.
39. Kim, D.J. *et al.* (2016) Herbacetin is a novel allosteric inhibitor of ornithine decarboxylase with antitumor activity. Cancer Res., 76, 1146–1157.
40. Qiao, Y. *et al.* (2013) Herbacetin induces apoptosis in HepG2 cells: involvements of ROS and PI3K/Akt pathway. Food Chem. Toxicol., 51, 426–433.
41. Berman, H.M. *et al.* (2000) The protein data bank. Nucleic Acids Res., 28, 235–242.
42. Pettersen, E.F. *et al.* (2004) UCSF chimera–a visualization system for exploratory research and analysis. J. Comput. Chem., 25, 1605–1612.
43. Lee, K.W. *et al.* (2011) Molecular targets of phytochemicals for cancer prevention. Nat. Rev. Cancer, 11, 211–218.
44. The Alpha-Tocopherol, Beta Carotene Cancer Prevention Study Group.(1994) The effect of vitamin E and beta carotene on the incidence of lung cancer and other cancers in male smokers. N. Engl. J. Med., 330, 1029–1035.
45. Lippman, S.M. *et al.* (2009) Effect of selenium and vitamin E on risk of prostate cancer and other cancers: the selenium and vitamin E Cancer Prevention Trial (SELECT). JAMA, 301, 39–51.
46. Omenn, G.S. *et al.* (1996) Effects of a combination of beta carotene and vitamin A on lung cancer and cardiovascular disease. N. Engl. J. Med., 334, 1150–1155.
47. Crowell, J.A. *et al.* (2007) Targeting the AKT protein kinase for cancer chemoprevention. Mol. Cancer Ther., 6, 2139–2148.
48. Nowotarski, S.L. *et al.* (2015) Skin carcinogenesis studies using mouse models with altered polyamines. Cancer Growth Metastasis, 8(Suppl 1), 17–27.
49. Jansen, A.P. *et al.* (2001) Relation of the induction of epidermal ornithine decarboxylase and hyperplasia to the different skin tumor-promotion susceptibilities of protein kinase C alpha, -delta and -epsilon transgenic mice. Int. J. Cancer, 93, 635–643.
50. Eferl, R. *et al.* (2003) AP-1: a double-edged sword in tumorigenesis. Nat. Rev. Cancer, 3, 859–868.
51. Madrid, L.V. *et al.* (2001) Akt stimulates the transactivation potential of the RelA/p65 subunit of NF-kappa B through utilization of the Ikappa B kinase and activation of the mitogen-activated protein kinase p38. J. Biol. Chem., 276, 18934–18940.